© 2016. Published by The Company of Biologists Ltd | Development (2016) 143, 3491-3505 doi:10.1242/dev.134882

STEM CELLS AND REGENERATION

RESEARCH ARTICLE

Beryllium nitrate inhibits fibroblast migration to disrupt epimorphic regeneration

Adam B. Cook and Ashley W. Seifert*

ABSTRACT

Epimorphic regeneration proceeds with or without formation of a blastema, as observed for the limb and skin, respectively. Inhibition of epimorphic regeneration provides a means to interrogate the cellular and molecular mechanisms that regulate it. In this study, we show that exposing amputated limbs to beryllium nitrate disrupts blastema formation and causes severe patterning defects in limb regeneration. In contrast, exposing full-thickness skin wounds to beryllium only causes a delay in skin regeneration. By transplanting full-thickness skin from ubiquitous GFP-expressing axolotls to wild-type hosts, we demonstrate that beryllium inhibits fibroblast migration during limb and skin regeneration *in vivo*. Moreover, we show that beryllium also inhibits cell migration *in vitro* using axolotl and human fibroblasts. Interestingly, beryllium did not act as an immunostimulatory agent as it does in Anurans and mammals, nor did it affect keratinocyte migration, proliferation or re-epithelialization, suggesting that the effect of beryllium is cell type-specific. While we did not detect an increase in cell death during regeneration in response to beryllium, it did disrupt cell proliferation in mesenchymal cells. Taken together, our data show that normal blastema organogenesis cannot occur without timely infiltration of local fibroblasts and highlights the importance of positional information to instruct pattern formation during regeneration. In contrast, non-blastemal-based skin regeneration can occur despite early inhibition of fibroblast migration and cell proliferation.

KEY WORDS: Beryllium, Regeneration, Wound healing, Limb development, *Ambystoma mexicanum*, Blastema

INTRODUCTION

Urodeles (salamanders and newts) are unique among tetrapods for their almost limitless ability to regenerate complex tissues and organs, including an entire limb (Butler and Ward, 1967; Wallace, 1981; Eguchi et al., 2011). Amazingly, this ability is not restricted to a single regeneration event, as repeated bouts of newt limb amputation continuously produce new limbs (Spallanzani, 1769). This example underscores the robust nature of regeneration and hints at the importance of local cells to continually divide and supply the raw material to faithfully restore a functional appendage. Limb regeneration in Urodeles represents an example of blastemal-based epimorphic regeneration whereby cells aggregate at the injury site to form a blastema, a transient mass of lineage-restricted progenitor cells that undergo proliferation, organogenesis and growth (Morgan, 1901; Chalkley, 1954; Endo et al., 2004; Kragl et al., 2009). Correct blastema patterning and growth are absolutely required for successful regeneration following amputation. In contrast, skin regeneration does not appear to require a blastemal intermediate (Seifert et al., 2012; Seifert and Maden, 2014). Instead, local fibroblasts migrate into the wound bed, undergo some proliferation and secrete an extracellular matrix (ECM) that directly remodels into the new dermis as the epidermis regenerates and makes new glands (Seifert et al., 2012).

Despite the robust nature of epimorphic regeneration, there are four classically defined methods to inhibit appendage regeneration: (1) severing the nerve supply, (2) removing or replacing the wound epidermis, (3) disrupting positional information and (4) inhibiting proliferation. There is a large body of literature documenting the requirement for nerves during regeneration (reviewed in Singer, 1952; Stocum, 2011). These studies have shown that when nerves are severed prior to limb amputation, a blastema fails to develop and regeneration does not occur (Todd, 1823; Schotté and Butler, 1941; Singer, 1951; Brockes, 1987). The effect of denervation, however, is not permanent since axons regrow into the limb stump a short time after the procedure and re-amputation of this previously denervated limb will lead to normal regeneration (Salley and Tassava, 1981). Innervation is required during blastema formation to promote the formation of a functional wound epidermis that secretes mitogenic factors to stimulate blastemal cell proliferation (Globus and Vethamany-Globus, 1977; Globus et al., 1980). Once the blastema reaches a critical mass, a neurotrophic factor is still required to maintain cellular mitosis until cell differentiation begins (Singer, 1952). The importance of the wound epidermis has been revealed through numerous studies showing that its removal, replacement or irradiation inhibits regeneration (Stocum and Dearlove, 1972; Mescher, 1976; Lheureux and Carey, 1987).

Dermal fibroblasts play a fundamental role during blastema formation and contain essential patterning information required for limb regeneration (Lheureux, 1975a,b, 1977; Muneoka et al., 1986; Bryant and Gardiner, 1989; Satoh et al., 2007). Following an injury and peak inflammatory response, fibroblasts migrate to the wound site, interact locally (with each other and inflammatory cells) and begin depositing ECM to support regeneration (Onda et al., 1990; Calve et al., 2010; Seifert et al., 2012). The interaction of cells from different positions (i.e. dorsal, ventral, anterior, posterior) is required for proper blastema formation (Carlson, 1974; Lheureux, 1975a,b; Stocum, 1978; Kim and Stocum, 1986; Ludolph et al., 1990). Migration of cells with intact positional information stimulates proliferation and organogenesis of the new limb. Creating abnormal dorsal-ventral or anterior-posterior interactions can cause aberrations in regeneration, ranging from supernumerary limbs to the complete inhibition of regeneration (Lheureux, 1975a, 1977; Bryant, 1976; Maden, 1983; Slack, 1983).

In addition to the nervous control of cell proliferation, irradiation and various chemical and molecular inhibitors have been used to demonstrate that cell proliferation is required during epimorphic

Department of Biology, University of Kentucky, Lexington, KY 40506, USA.

*Author for correspondence (awseifert@uky.edu)

A.W.S., 0000-0001-6576-3664

Received 7 January 2016; Accepted 12 August 2016

Development (2016) 143, 3491-3505 doi:10.1242/dev.134882

regeneration in Urodeles (Thornton, 1943; Singer et al., 1956; Sobell, 1985; Singh et al., 2012). The inhibitory effects of irradiation on appendage regeneration have been well documented (Maden and Wallace, 1976). Irradiation of an uninjured limb such that mesenchymal cells (along with epidermal cells) are exposed followed by amputation completely inhibits regeneration (Maden and Wallace, 1976). Thornton (1943) demonstrated that colchicine can inhibit limb regeneration in larval salamanders, and this was later shown to result from colchicine-induced nerve damage and inhibited cellular proliferation (Singer et al., 1956). More recently, it was shown that cyclopamine inhibition of hedgehog signaling during newt limb regeneration reduces blastemal cell proliferation, which causes severe patterning defects (Singh et al., 2012).

In 1949, C. S. Thornton demonstrated that briefly exposing freshly amputated limbs to the alkaline earth metal beryllium, completely inhibits limb regeneration in larval marbled salamanders (*Ambystoma opacum*) whereas the contralateral limb regenerates normally (Thornton, 1949). Beryllium is the only alkali or alkaline earth metal that specifically inhibits regeneration without disrupting normal physiological function (Needham, 1941). A recent study using *Xenopus* suggests that beryllium acts as a potentiator of inflammation to inhibit larval limb regeneration in Anurans, while another study suggests that beryllium inhibits limb regeneration by antagonizing the PIP3 inositol pathway and subsequent proliferation (Tsonis et al., 1991; Mescher et al., 2013). Here, we investigate how beryllium inhibits blastema-based regeneration using axolotl (*Ambystoma mexicanum*) limb amputation as a model system. In addition, we also test the hypothesis that beryllium similarly affects blastema-independent regeneration using a full-thickness excisional skin wound model (Seifert et al., 2012).

RESULTS

In order to investigate the effect of beryllium on regenerative ability, we first sought to replicate previous experiments showing that a short exposure to beryllium completely inhibits limb regeneration (Thornton, 1949, 1950, 1951). Replicating the originally published parameters and substituting juvenile axolotls (*Ambystoma mexicanum*) for *Ambystoma opacum* larvae, we found that limb regeneration was severely perturbed, but not completely inhibited in response to beryllium nitrate (BeN) exposure (Fig. 1). Examining control limbs after amputation, every animal formed a blastema and ultimately regenerated a new limb (Fig. 1A-C). In contrast, BeN-treated limbs formed a small edema at the amputation plane, which persisted until control limbs had already formed digits (Fig. 1D). Obvious blastema or cone stages were rarely observed by light microscopy in treated limbs. Upon analyzing BeN treated limbs 98 days after injury (D98), we observed very small, mispatterned limbs that were well-vascularized (Fig. 1E). By D200, some melanocytes had migrated distally, but limbs remained heteromorphic (Fig. 1F). We noted that melanocyte migration was always disrupted distally (Fig. 1E,F). To more fully understand the extent to which BeN affected patterning during regeneration we analyzed skeletal preparations from control and treated limbs (Fig. 1G-J and Table S1). While control limbs almost always regenerated the complete compliment of amputated structures, including stylopod, zeugopod and autopod, 94.7% of treated limbs displayed patterning defects (Fig. 1G-I and Table S1). All treated limbs, regardless of defect, were smaller compared with control limbs and the patterning defects were more severe proximally in ~70% of treated limbs (Fig. 1G-I and Table S1). Proximal defects were associated with a stunted humerus, loss or fusion of the elbow to the radius/ulna, loss or fusion or duplication of the radius and ulna and altered carpal number (Fig. 1G-I and Table S1). Digit number was also variable in BeN-treated limbs, ranging from 1 to 5 digits (Fig. 1G-I and Table S1). We followed some animals for up to 2 years after BeN exposure and observed no adverse health effects, supporting previous assertions that beryllium inhibited regeneration locally, rather than altering whole organism physiology (Thornton, 1949).

In order to investigate how beryllium might inhibit non blastemal-based regeneration, we turned to a full-thickness skin wound. Our previous work showed that pedomorphic axolotls completely regenerate a 4 mm full-thickness excisional skin wound in 80 days (Seifert et al., 2012) and we observed a similar time course during our experiments. We compared BeN-treated skin wounds with control wounds and noted several important defects (Fig. 2A-H). At D14, BeN-treated wounds showed a similar response to BeN-treated limbs and were notable for a lack of pigment cells migrating into the wound, persistent presence of edema and increased wound size compared with the original wound area (Fig. 2A,B). By D21, control wounds were significantly smaller than BeN-treated wounds (9.93±0.91 mm^2 and 28.77±2.82 mm^2, respectively; t=5.64, P<0.005) (Fig. 2I). In fact, wound area in BeN-treated wounds had more than doubled compared with the original wound area (original wound, 12.57 mm^2; D21 BeN-treated wound area, 28.77±2.82 mm^2). Whereas the original wound was difficult to visualize at D64 in control samples, treatment wounds were still visible at this time point, but became harder to detect by D80 (Fig. 2E-H). These results suggest that BeN exposure inhibits wound contraction following injury.

In order to ascertain if beryllium affected re-epithelialization during regeneration, we next examined the cellular structure of healing wounds and found that keratinocytes re-epithelialized treatment and control wounds in 24 h (Fig. 2J). A thin layer of keratinocytes and Leydig cells covered all wounds within 24 h of injury and wounding elicited a typical hemostatic response (Fig. 2J). While blood cells were present in treatment and control wounds, a large number of erythrocytes and plasma persisted in BeN-treated wounds until D21 (Fig. 2B,D and Fig. 3). While we detected collagen in control wounds beginning at D14, collagen deposition was not detected in treatment wounds until after D21 (Fig. 3). In D42 control wounds, the regenerating dermis began stratifying into an upper stratum spongiosum and lower stratum compactum, and new glands regenerating from the epidermis were evident (Fig. 3). By D80, skin in control wounds had completely regenerated and resembled unwounded skin (Fig. 3). In contrast, D42 BeN-treated wounds developed a dense dermal ECM layer associated with the basement membrane and no regenerating glands were present (Fig. 3). Surprisingly, D80 wounds in BeN-treated skin resembled D42 control wounds, whereby the collagen-rich dermal layer began subdividing and new glands were evident descending from the epidermis (Fig. 3). At D139, there was little noticeable difference between treatment and control wounds. Together, these data demonstrated that BeN exposure delayed, but did not inhibit skin regeneration.

Our observation of reduced collagen deposition following BeN treatment led us to ask whether other components of the extracellular matrix (ECM) normally deposited during skin regeneration were similarly affected (Seifert et al., 2012). Analyzing wound-bed tissue at D14, we found that Fibronectin-1 (FN1) and Tenascin-C (TNC) were deposited throughout the regenerating dermis (Fig. 4). We also used Alcian Blue to show glycosaminoglycan (GAG) production, which we detected throughout the wound bed in control skin (Fig. 4). In contrast to control-treated wounds, FN1 and TNC were barely

Development (2016) 143, 3491-3505 doi:10.1242/dev.134882

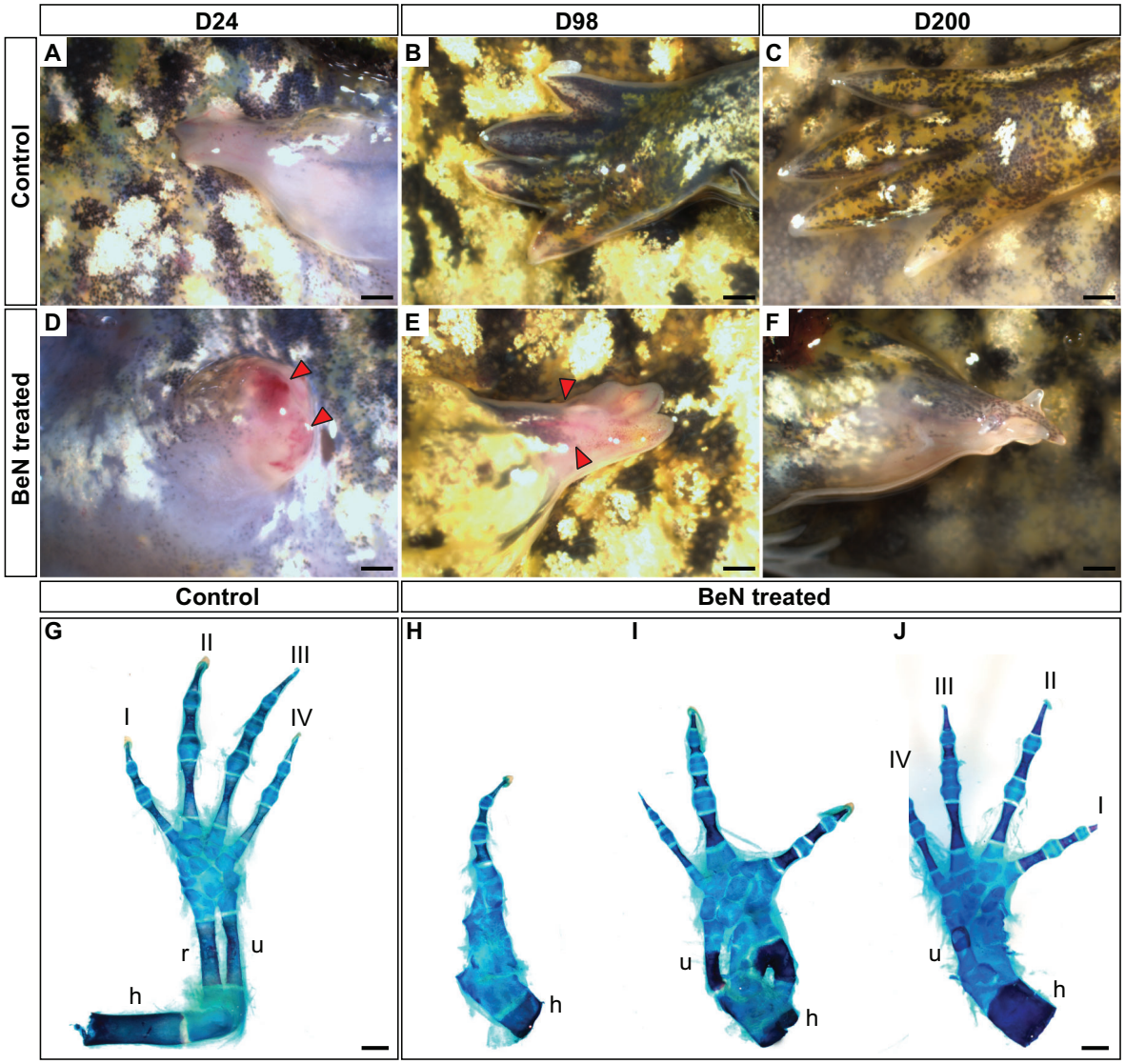

Fig. 1. BeN treatment disrupts blastema formation and alters patterning during axolotl limb regeneration. Amputated limbs treated with BeN were imaged during regeneration alongside contralateral control limbs. (A,D) D24, control limbs showed normal differentiation of the digits, while BeN-treated limbs showed an edema (red arrows) with no signs of blastema formation (D). (B) Untreated limbs had completely regenerated by 98 days. (E) D98 BeN-treated limbs exhibited patterning defects and reduced melanocyte migration into the regenerate (red arrows). Compared with control limbs at D200 (C), BeN-treated limbs showed permanent malformations including truncated proximal distal outgrowth, atypical digit formation and reduced melanocyte numbers (F). (G-J) Skeletal preparations of contralateral control (G) and treated limbs (H-J). Treated limbs showing spectrum of defects resulting from BeN treatment, where ~70% of animals exhibited more severe proximal malformations. Although at least one digit (roman numerals in G,J) formed in all treated limbs, 78.9% of treated animals had defects in the elbow (H-J), fusions of the radius/ulna (H,J), duplications of the radius or ulna (I,J) and/or carpal malformation (H-J). For whole-mount images, data is representative of n=5/group/day and for skeletal preparations n=19/group. h, humerus; r, radius; u, ulna. Scale bars: 1 mm.

detectable in BeN-treated wounds (Fig. 4). Similarly, GAGs were not present in the wound bed of the treatment group at D14 (Fig. 4). Together with our histological observations, these results indicate that BeN inhibits ECM deposition (directly or indirectly) and this is associated with a delay in the normal time course of skin regeneration.

A lack of ECM production in BeN-treated wounds suggested three hypotheses: (1) a persistent inflammatory response prevented progression to a regenerative response; (2) fibroblasts were dying and thus not able to produce new ECM; or (3) fibroblasts were not migrating into the wound bed. We first tested if BeN treatment increased cellular inflammation in the wound bed by assessing leukocyte numbers using an antibody against L-plastin, a pan-leukocytic marker (Jones et al., 1998; Seifert et al., 2012) (Fig. 5). Calculating the percentage of L-plastin$^+$ cells that infiltrated into the wound bed following injury, we did not find significant differences between BeN-treated and control wounds at any day examined: D3, 43.60±3.72% and 42.19±9.57%, t=0.14, P=0.8985; D7, 25.16±7.05% and 37.72±6.28%, t=−2.13, P=0.0999; D10, 11.30±2.09% and 16.77±4.49%, t=−1.95, P=0.1229 for treatment and control, respectively) (Fig. 5A-D). We also examined leukocyte infiltration past the amputation plane in control and BeN-treated limbs (Fig. 5E-H). We counted L-plastin$^+$ cells during late blastema stage and cone stages, which was determined by the progression of the contralateral untreated limb to these stages. We observed a small, but significant decrease in L-plastin$^+$ cells in BeN-treated versus control regenerated tissue at the late blastema stage (4.63±0.80% and 6.88±1.17%, respectively; t=−3.19, P=0.0333) (Fig. 5E,F).

Development (2016) 143, 3491-3505 doi:10.1242/dev.134882

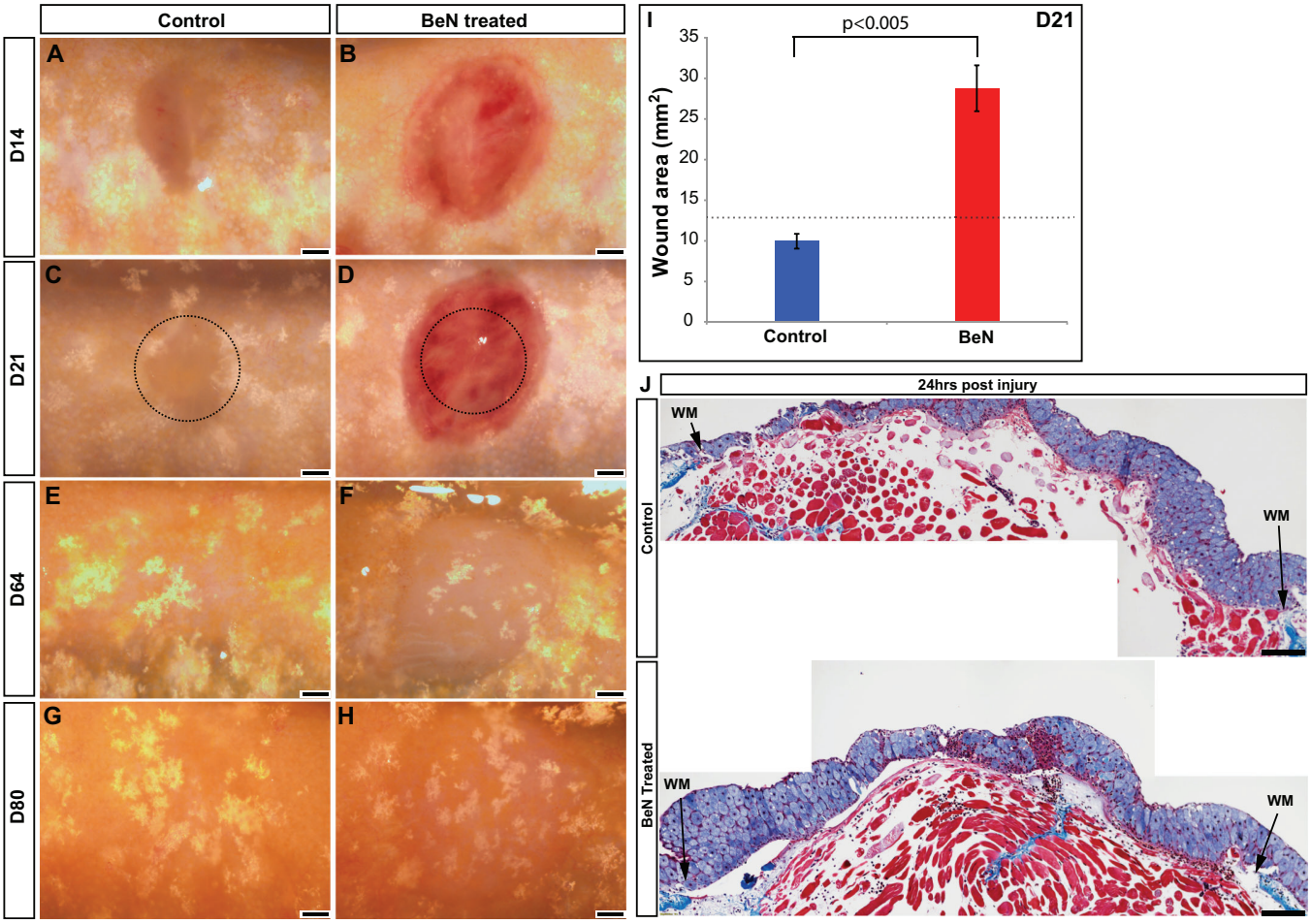

Fig. 2. BeN inhibits wound contraction and delays pigment cell migration, but not epidermal cell migration in axolotls. (A-H) Full-thickness excisional wounds were followed for 80 days. (A,C) Control wounds contracted during the first 21 days. (B,D) BeN-treated wounds expanded from initial biopsy area and retained large numbers of blood cells through D21. Dotted circles show original wound area (C,D). (E,F) Pigment cell (iridophore) migration was reduced in treated wounds. (G,H) D80 control wounds were indistinguishable from the surrounding unwounded tissue, while treated wounds maintained a clearly defined wound edge with dermal tissue and muscle still visible through the epidermis. (I) The mean area of treated wounds at D21 was three times larger than control (control, 9.93±0.91 mm^2; treatment, 28.79±2.82 mm^2; P<0.005; mean±s.e.m.). (J) Epidermis covered the entire wound surface in both treatment and control wounds after 24 h. BeN-treated wounds appeared to have portions of the epidermis in which densely packed erythrocytes interrupted the contiguous layer of Leydig cells. Data representative of n=5/group/day. WM, wound margin. Scale bars: 1 mm.

Although the percentage of L-plastin$^+$ cells remained decreased at the cone stage, it was not significantly lower (3.40±1.29% and 10.2±3.00%, respectively; t=−1.85, P=0.1620) (Fig. 5G,H). These data clearly show that BeN does not stimulate increased inflammatory cell influx into dorsal skin wounds or into regenerating limb tissues, although erythrocytes and plasma persist longer in the wound bed in BeN-treated wounds.

Dermal fibroblasts are the primary cell type involved in blastema formation (Gardiner et al., 1986, Muneoka et al., 1986) and are responsible for producing new ECM during limb and skin regeneration (Gulati et al., 1983; Onda et al., 1990; Asahina et al., 1999; Calve et al., 2010; Seifert et al., 2012). The relative absence of ECM proteins in the wound bed of BeN-treated wounds suggested that fibroblasts might be absent from the wound bed, either because they failed to migrate into the wounds or because they failed to survive after BeN exposure. In order to label and follow migrating cells during regeneration, we took advantage of a transgenic axolotl line in which all cells constitutively express GFP (Sobkow et al., 2006). We transplanted full-thickness (epidermis and dermis) GFP$^+$ dorsal skin onto wild-type (WT) host flanks (whose cells do not express GFP), allowed the grafts to heal, and then made wounds in the grafts to track cell migration into the wound bed (Fig. 6A-D). We counted GFP$^+$ cells at D14 when large numbers of fibroblasts are normally observed in the wound bed and ECM molecules are readily detectable (Figs 3 and 4). We found significantly more GFP$^+$ cells in control compared with BeN-treated wounds (5.66±1.9% and 0.33±0.11% GFP$^+$ cells, respectively; t=−6.44, P<0.0001) (Fig. 6B-D).

We also analyzed fibroblast migration into regenerating limbs by grafting full-thickness posterior skin cuffs from GFP$^+$ individuals onto WT host forelimbs (Fig. 6E). After grafting, we allowed the grafts to heal for 14 days, amputated the left limb through the center of the GFP graft, treated this limb with BeN, then amputated the right (control) limb and tracked GFP$^+$ fibroblasts during limb regeneration (Fig. 6F,G). After harvesting limbs at late blastema and cone stages based on control limbs, we observed significant migration of GFP$^+$ fibroblasts out of the dermis, past the amputation plane and towards the distal tip of the blastema (Fig. 6F). BeN-treated limb equivalents showed some GFP$^+$ cells deep within the stump beneath the dermis in unwounded tissues; however, only a

Development (2016) 143, 3491-3505 doi:10.1242/dev.134882

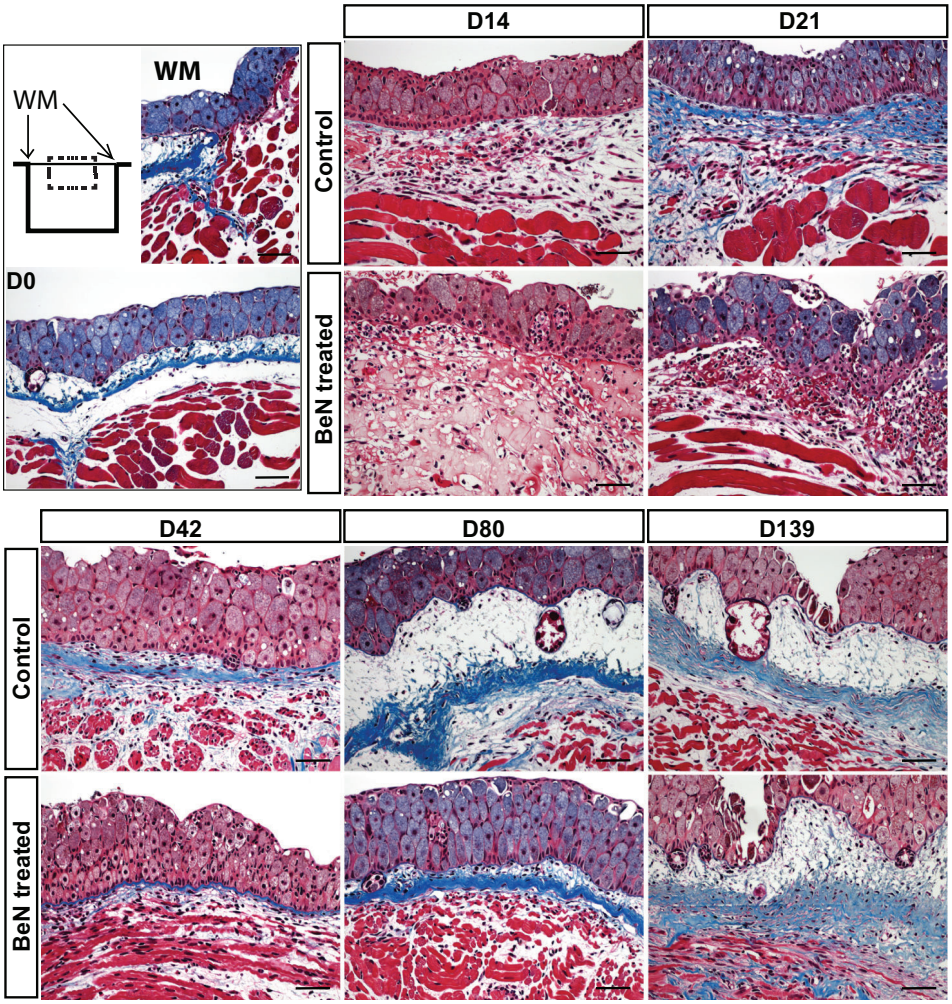

Fig. 3. BeN delays skin regeneration in axolotls. Masson's trichrome stained sections comparing control and BeN-treated full-thickness excisional wounds. Control wounds showed ECM deposition at D14. BeN-treated wounds showed delayed ECM deposition until D42. ECM deposited at D42 was tightly bundled and localized near the basal lamina. Gland regeneration was apparent in control wounds at D42 and appeared at D80 in treated wounds (yellow arrows). Full-thickness skin (dermis and epidermis) in control wounds had completely regenerated by D80 and resembled unwounded tissue. Skin regeneration was delayed in treated wounds, with dermis and epidermis mostly regenerated by D139. Images represent center of the wound bed. Blue, collagen; red, muscle; purple, cytosol; black, nucleus. Data representative of *n*=5/group/day. WM, wound margin. Scale bars:100 µm.

few, loosely scattered GFP^+ cells were present past the amputation plane (Fig. 6G). To address the possibility that BeN treatment might affect re-innervation and wound epidermis formation, we assessed axon migration into control and BeN-treated wounds (Fig. S1). We found labeled axons beneath the nascent blastema in BeN-treated limbs as well as axons innervating the smaller blastemas at later time points (and the wound epidermis) (Fig. S1). Lastly, we performed a TUNEL assay on tissue harvested from control and BeN-treated wounds at D1, D3 and D7 to test whether BeN treatment induced cell death and found no significant difference between groups at any time point (F=0.5668, P=0.5845) (Fig. 7A-C). Taken together, our data show that BeN treatment primarily affects cell migration (either directly or indirectly) and did not induce cell death within the wound.

While our transplant experiment demonstrated that cells failed to move into the wound bed, we could not rule out the possibility that beryllium exposure might affect production of a chemotactic factor, either from the epidermis or from other cells within the wound bed. To directly test the effect of BeN on fibroblast cell migration, we cultured axolotl AL1 cells (an axolotl fibroblast line) and exposed them to three concentrations of BeN to determine a concentration that did not induce cell death, thus mimicking our *in vivo* results (see Materials and Methods). Based on these experiments we found that 10 mM BeN did not induce significant cell death *in vitro*. To assess migratory ability of cultured cells, we created an *in vitro* wound using a round sterile applicator in the center of each well of a 12-well plate. Following cells every 24 h, we noted that control cells began migrating into the *in vitro* wound on D2. By D14, large numbers of control cells had migrated into the wound center (Fig. 8). In stark contrast, by D14 we found that few BeN-treated fibroblasts had migrated into the circular wound (Fig. 8). Because we conducted the assay at ∼70-80% confluency, we assessed confluency outside the scratch at D14 and found that cells were 100% confluent in control and treatment groups, suggesting that BeN did not significantly inhibit cell division (Fig. 8).

Based on our findings in salamanders, we were curious if beryllium similarly affected mammalian cells and asked if BeN treatment altered the migratory ability of human dermal fibroblast (hADF) cells (Fig. 9). We performed the same *in vitro* assay as above and followed hADF cells every 12 h because mammalian cells divide much more quickly than axolotl cells (Fig. 9). Similar to axolotl AL1 cells, we found that a 10 mM treatment with BeN reduced cell migration into scratch wounds. Untreated hADF cells successfully migrated and completely filled an *in vitro* wound by 96 h (Fig. 9). Few BeN-treated cells migrated into the scratched area by 96 h and the area remained largely uninhabited by cells, even 15 days after treatment (Fig. 9 and data not shown). We also noted a tendency of BeN-treated hADF cells to ball up (Fig. 9). Examining cells outside the scratched areas, we noted that while control wells reached 100% confluency, cells in treated wells remained at ∼70% confluency, suggesting limited cell growth of mammalian cells (Fig. 9).

Development (2016) 143, 3491-3505 doi:10.1242/dev.134882

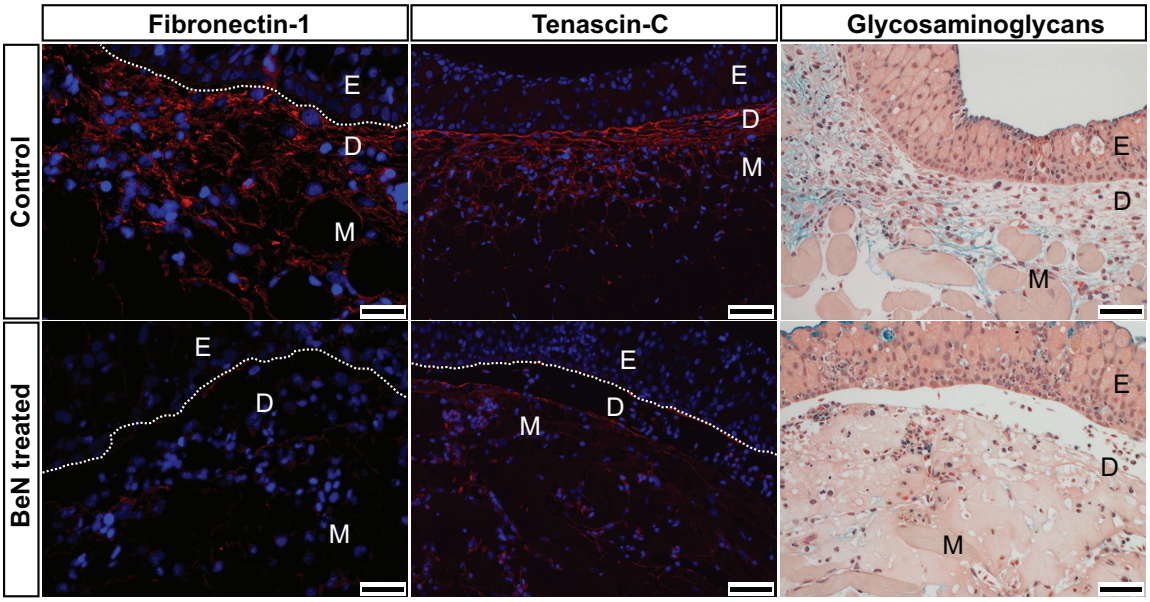

Fig. 4. BeN inhibits early deposition of extracellular matrix (ECM) proteins. Panels represent cross sections of full-thickness skin showing epidermis (E), dermis (D) and muscle (M) in control and BeN-treated wounds at D14. Fibronectin-1, Tenascin-C and glycosaminoglycans (GAGs) are visible in the wound bed of controls, but are absent from BeN-treated wounds. GAGs were visualized with Alcian Blue. Scale bars: 50 µm (Fibronectin), 100 µm (Tenascin-C and GAGs). Dotted white lines show boundary of epidermis and dermis. Data are representative of n=5/group.

Although it appeared that AL1 fibroblasts continued growing after BeN treatment, the failure to reach confluency in hADF cells suggests that BeN might affect cell cycle progression. Thus, we used flow cytometry to calculate the relative fraction of cells in each phase of the cell cycle and test if BeN disrupted cell cycle progression. Following control or BeN treatment, we allowed AL1 cells to continue cycling for 48 h (equal to at least one complete cell cycle) (Wallace and Maden, 1976; Maden, 1978) before performing flow analysis based on DNA content (Table 1). We found that BeN significantly altered cell cycle progression (χ^2=7.34, P=0.026) and a *post hoc* analysis indicated that BeN treatment led to a significant increase in the percentage of cells in S phase and a significant decrease in G2/M phase cells (Table 1). The percentage of cells in G0/G1, however, was not different between treatment and control (Table 1). This suggested that BeN treatment was delaying or blocking the transition to G2/M in axolotl fibroblasts. We also analyzed hADF cells and found that BeN disrupted the mammalian cell cycle (χ^2=62.55, P=0.00001) (Table 1). In contrast to AL1 cells, we found a 20% increase in the percentage of cells in G0/G1, whereas we observed a decrease in the percentage of cells in S phase and G2/M, (Table 1). This data suggests that BeN affects cell cycle progression, albeit differently in axolotl versus human cells.

Based on our *in vitro* results, we used EdU to analyze cells progressing through S phase in regenerating limbs following control or BeN treatment during early blastema, mid blastema and palette stages (Fig. 10A). We found that BeN treatment reduced the proliferative index during time points corresponding to blastema stages, but not during the palette stage, when cells were differentiating in control limbs (F=4.4, P=0.037) (Fig. 10A). Among control limbs, there was no difference in proliferative index between the observed stages (F=0.60, P=0.57). The difference in proliferative index observed in response to BeN treatment between blastema stages and the palette stage were driven by an increase in the number of EdU^+ cells (F=9.4, P<0.005), as the average cell density in BeN-treated limbs was not different across stages (F=1.9, P=0.19). We obtained a similar result comparing $BrdU^+$ dermal cells between BeN-treated and control skin wounds (Fig. 10B-D). The proliferative index of dermal cells in BeN-treated wounds was significantly reduced at D7 and D14 post injury (D7, t=−4.86, P=0.008; D14, t=−3.36, P=0.028). We also analyzed keratinocyte proliferation and found no difference in the proliferative index when comparing BeN-treated and control epidermis (D7, t=−1.09, P=0.337; D14, t=1.92, P=0.127) (Fig. 10E-G). These data support our *in vitro* findings with AL1 cells where beryllium treatment leads to an accumulation of cells in S-phase, but also show that BeN does not affect keratinocytes.

DISCUSSION

Our results provide a cellular mechanism to explain the inhibitory effect of beryllium on regeneration in salamanders. We found that BeN inhibited the ability of local fibroblasts to migrate in response to injury and this, in turn, disrupted regeneration. We also found that beryllium disrupts cell cycle progression *in vivo* and *in vitro*. While limb regeneration was permanently affected, we found that a similar application of BeN to full-thickness skin injuries only delayed skin regeneration. These results reveal that timely migration of fibroblasts in response to injury is necessary for proper blastema organogenesis during epimorphic regeneration, while this early migration event is not necessary in the absence of a blastema (i.e. skin regeneration). Despite inhibiting local fibroblasts from migrating into skin injuries, some fibroblasts eventually invade the wound bed and facilitate normal dermal regeneration. Importantly, our observations of severe patterning defects (loss of elements or duplications) in BeN-treated limbs supports the importance of cell-cell interactions during limb regeneration and highlights beryllium as a potential tool to further investigate positional identity.

Although they were difficult to observe macroscopically, blastemas eventually formed in BeN-treated limbs and were smaller compared with control limb blastemas. We found axons present beneath the wound epidermis in BeN-treated limbs and cell proliferation reached comparable levels to untreated limbs during

Development (2016) 143, 3491-3505 doi:10.1242/dev.134882

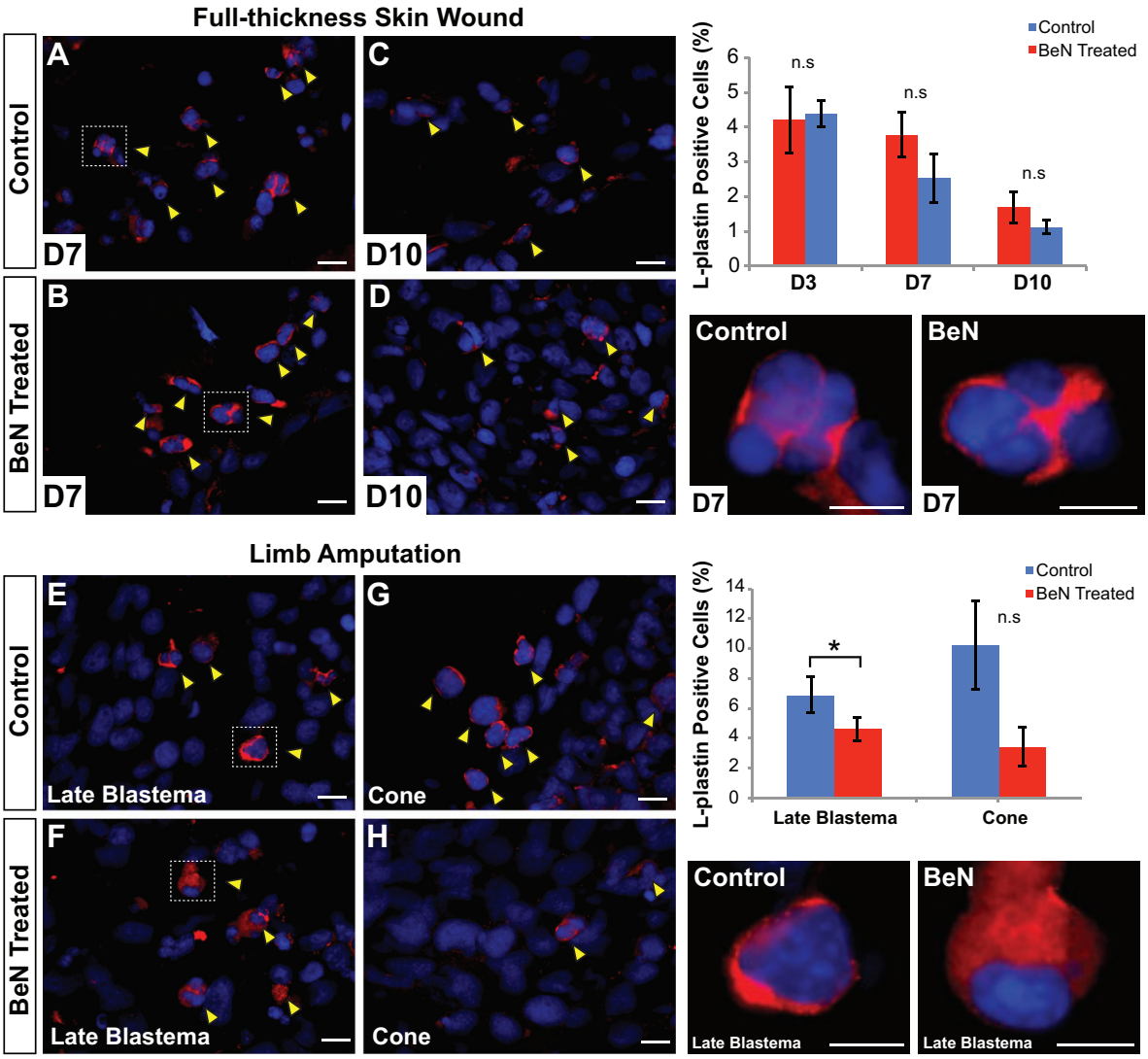

Fig. 5. Leukocyte infiltration is not affected in BeN-treated skin wounds and is slightly reduced in BeN-treated limbs. Axolotl skin wounds were harvested at D3, D7 and D10, and leukocytes were detected with the pan-leukocytic marker L-plastin. (A-D) Representative images showing L-plastin$^+$ cells beneath the epidermis in control and BeN-treated wounds at D7 (A,B) and D10 (C,D). Top graph shows that control and treatment wounds have similar levels of L-plastin$^+$ cells beneath the epidermis at all time points. High magnification images of boxed regions in A,B show morphology consistent with neutrophils and monocytes in L-plastin$^+$ cells at D7 in control and treated wounds. (E,G) L-plastin$^+$ cells were detected distal to the amputation plane of control limbs at late blastema and cone stages. BeN-treated limbs harvested at the same time as control limbs show a small, but significant (*P<0.05) reduction in L-plastin$^+$ cells at the late blastema stage (E,F and bottom graph). High magnification images of boxed regions in E,F show morphology consistent with leukocytes in L-plastin$^+$ cells at late blastema in control and treated limbs. While fewer L-plastin$^+$ cells were also detected past the amputation plane, at the equivalent cone-stage time in BeN-treated limbs, this difference was not significant (G,H and bottom graph). Data are representative of n=5/group, except cone stage, where n=4/group. Data are mean±s.e.m. Scale bars: 20 µm (A-D, E-H) and 10 µm in high-magnification images.

the differentiation stages of blastemal morphogenesis. Interestingly, the effect of beryllium appeared to be cell type-specific as epidermal cells and leukocytes migrated normally in the skin and limb. Despite axonal outgrowth in BeN-treated limbs we were unable to rule out the possibility of delayed Schwann cell migration, which could have contributed to a delay in blastema formation. However, our GFP transplant experiments tracking fibroblasts clearly show that beryllium inhibits local fibroblast migration and this *in vivo* data was supported by *in vitro* experiments using axolotl fibroblasts.

Dermal fibroblasts are necessary for limb regeneration and constitute up to 78% of early blastemal cells (Muneoka et al., 1986). Previous work has shown that fibroblasts contain stable positional information that is likely to be encoded in cell surface proteins and that the normal interaction of cells from disparate positions is required for blastema formation and proper limb patterning (Carlson, 1974; Lheureux, 1975a,b; Nardi and Stocum, 1984; Crawford and Stocum, 1988a,b; Echeverri and Tanaka, 2005; Kragl et al., 2009). Our results suggest that inhibiting fibroblast migration with beryllium interrupts the necessary interaction of cells from disparate positions and support fibroblast identity/interaction as an underlying cause of the observed patterning defects. That we eventually observed cells past the amputation plane suggests that some cells were capable of limited migration – an observation supported by our *in vitro* experiments. While the identity of these cells remains unclear, the range of skeletal malformations we observed suggests a random integration of cells from different positions. Given the unpredictable nature of cells ultimately

Development (2016) 143, 3491-3505 doi:10.1242/dev.134882

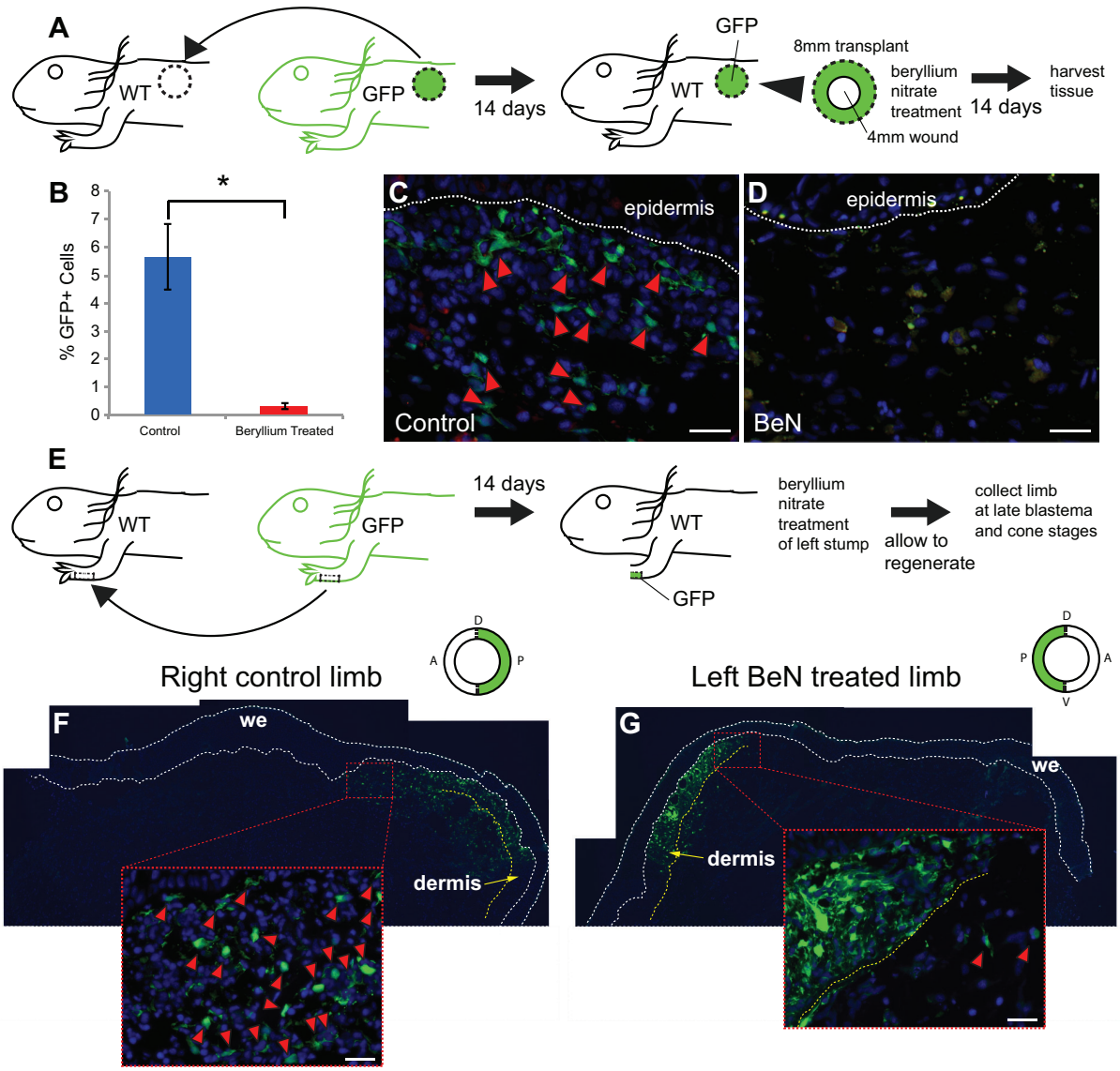

Fig. 6. BeN treatment severely reduces fibroblast migration into axolotl skin wounds and regenerating limbs. (A) Schematic depicting experimental paradigm for tracking GFP-labeled fibroblasts into skin wounds. Skin biopsies 8 mm thick containing epidermis and dermis were harvested from the dorsal flank of axolotls ubiquitously expressing GFP (n=5) and transplanted to 8 mm wound beds created on WT animals. Skin transplants were allowed to heal for 14 days after which a 4 mm full-thickness wound was made in the center of the transplant. BeN treatment occurred immediately following injury (see Materials and Methods). (B-D) Wound bed tissue harvested at D14. (B) Control wounds had significantly more GFP$^+$ cells compared with BeN-treated wounds (t=–6.44, P<0.0001; n=5/group). (C,D) Red arrows indicate GFP$^+$ cells. Few GFP$^+$ cells were detected in BeN-treated wounds. (E) Schematic depicting experimental paradigm for tracking GFP-labeled fibroblasts into amputated limbs (see Materials and Methods). Briefly, full-thickness skin cuffs (epidermis and dermis) from the posterior half of GFP limbs were transplanted to the corresponding position on WT limbs to preserve orientation. Limb cuffs were allowed to heal for 14 days and limbs were amputated through the center of the skin cuff. Regenerating limbs were harvested from control and BeN-treated limbs at late blastema stages (F,G). We observed significant migration of GFP$^+$ dermal fibroblasts (red arrows) beyond the amputation plane in control limbs deep into the stump and into the blastema (F and inset). In contrast, we observed very few GFP$^+$ dermal fibroblasts migrating beyond the amputation plane in BeN-treated wounds (G and inset). Dotted white lines depict bottom and top of epidermis and yellow dotted line represents the most ventral boundary of the dermis (F,G). Erythrocytes that were autofluorescent at both red and green wavelengths were not counted as GFP$^+$. Scale bars: 50 µm.

arriving in the blastema and proliferating, the resultant interactions produced cases indicative of this unpredictability: almost complete inhibition of regeneration and loss of elements in some cases and skeletal duplications with normal digit number in others. Interestingly, beryllium appeared to disproportionately affect proximal structures such that heteromorphic limbs never regenerated a complete/normal stylopod or zeugopod. In contrast, at least one digit formed, even in the most severe cases. Development of genetic markers for different positions in the limb will be necessary to definitively test our hypothesis concerning positional information, such that the identity of cells interacting past the amputation plane can be determined.

One concern with exposing organisms or cells to a highly reactive element like beryllium is the risk of disrupting basic cellular processes. We addressed this concern in three ways. First, we kept and observed animals treated with beryllium for over 2 years and noted that they grew normally and were capable of breeding. Second, although beryllium toxicity has been suggested to activate a caspase-dependent apoptotic pathway (Pulido and Parrish, 2003), we were able to assess apoptosis through TUNEL labeling and determine that

Development (2016) 143, 3491-3505 doi:10.1242/dev.134882

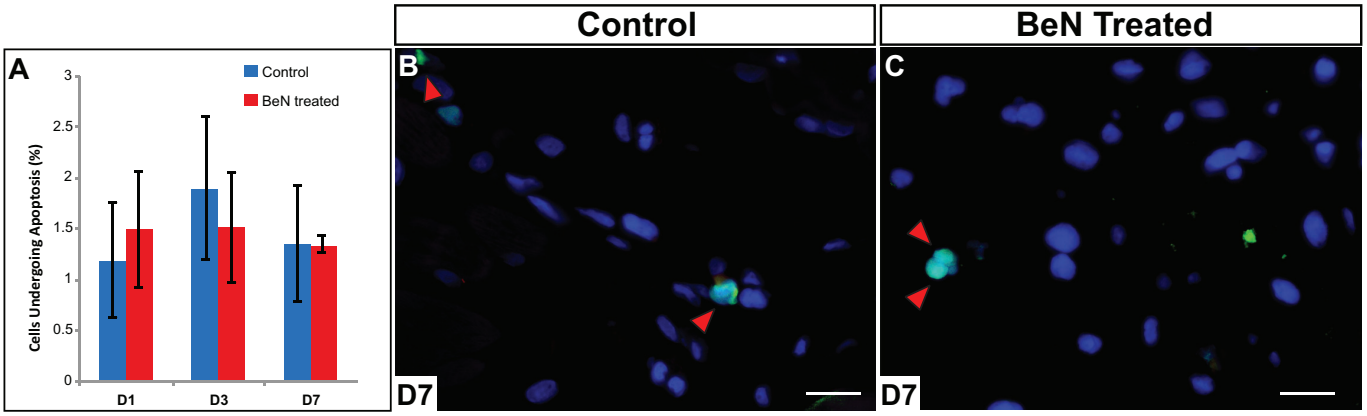

Fig. 7. BeN treatment does not affect cell death *in vivo*. TUNEL assay was used to detect dying cells in axolotl wound bed tissue. (A) The percentage (mean± s.e.m.) of dying cells was not different in control and BeN-treated skin wounds across all time points examined (two-way ANOVA, F=0.5668, P=0.5845; n=5/group/day). (B,C) Day 7 results shown as representative examples. Red arrows indicate TUNEL$^+$ cells. Yellow cells are autofluorescent in both red and green wavelengths and thus were not counted as GFP$^+$. Scale bars: 50 µm.

BeN exposure did not increase apoptosis *in vivo*. Our *in vitro* experiments used a concentration of BeN that inhibited cell migration without causing a detectable difference in cell death. Lastly, we quantified cell proliferation and cell cycle progression and found that beryllium exposure disrupted cell proliferation *in vivo* and *in vitro*. Examining axolotl fibroblasts *in vitro*, we found a small, but significant increase in S-phase cells and a decrease in the number of cells in G2/M-phase following BeN treatment. We obtained similar results *in vivo* by observing EdU incorporation and the proliferative index of limb mesenchyme following amputation. While the proliferative index of BeN-treated limb cells matched contralateral control limbs at later time points, this result was driven by an accumulation of EdU$^+$ cells, not an increase in cell density. Following BeN exposure *in vivo*, we also observed a transient reduction in cell proliferation in skin fibroblasts. Interestingly, keratinocyte proliferation was unaffected by BeN treatment, which supports a targeted, cell type-specific effect of beryllium. Experimental inhibition of cell proliferation during limb regeneration, either through chemical means or through removal of the wound epidermis, leads to precocious differentiation and formation of proximal

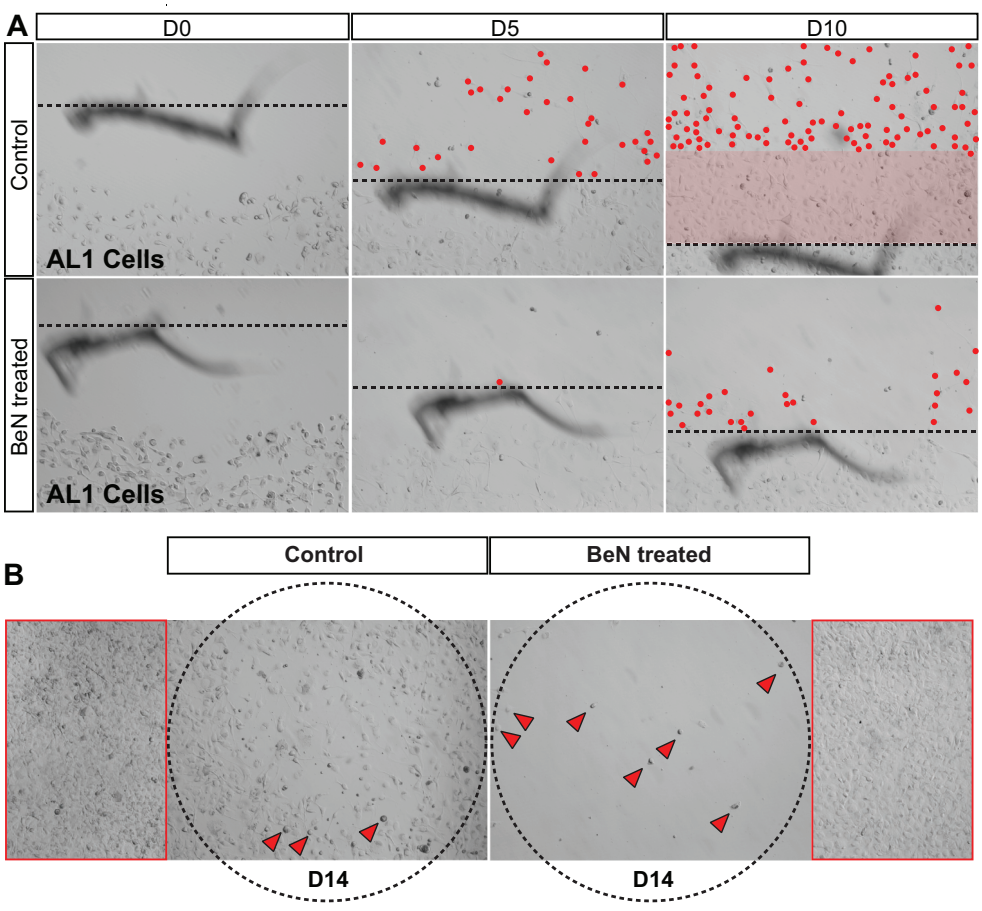

Fig. 8. BeN reduces migratory capabilities of axolotl AL1 cells *in vitro*. (A) Migration of AL1 fibroblasts across the inside edge (dotted line) of a circular scratch was tracked over the course of 10 days (red dots). The pink shaded box indicates an area >90% filled with cells. (B) BeN treatment inhibited migration of AL1 cells and reduced total migration distance. Dotted circle represents the original scratch area where untreated cells successfully migrated towards the center. Cell density was ~70-80% at treatment and cells in treated and control wells achieved confluency by D14 (red boxed areas). Red arrows indicate balled-up cells that were present in both treatment and control groups and did not stain with Trypan Blue (data not shown). Data representative of n=6/group.

Development (2016) 143, 3491-3505 doi:10.1242/dev.134882

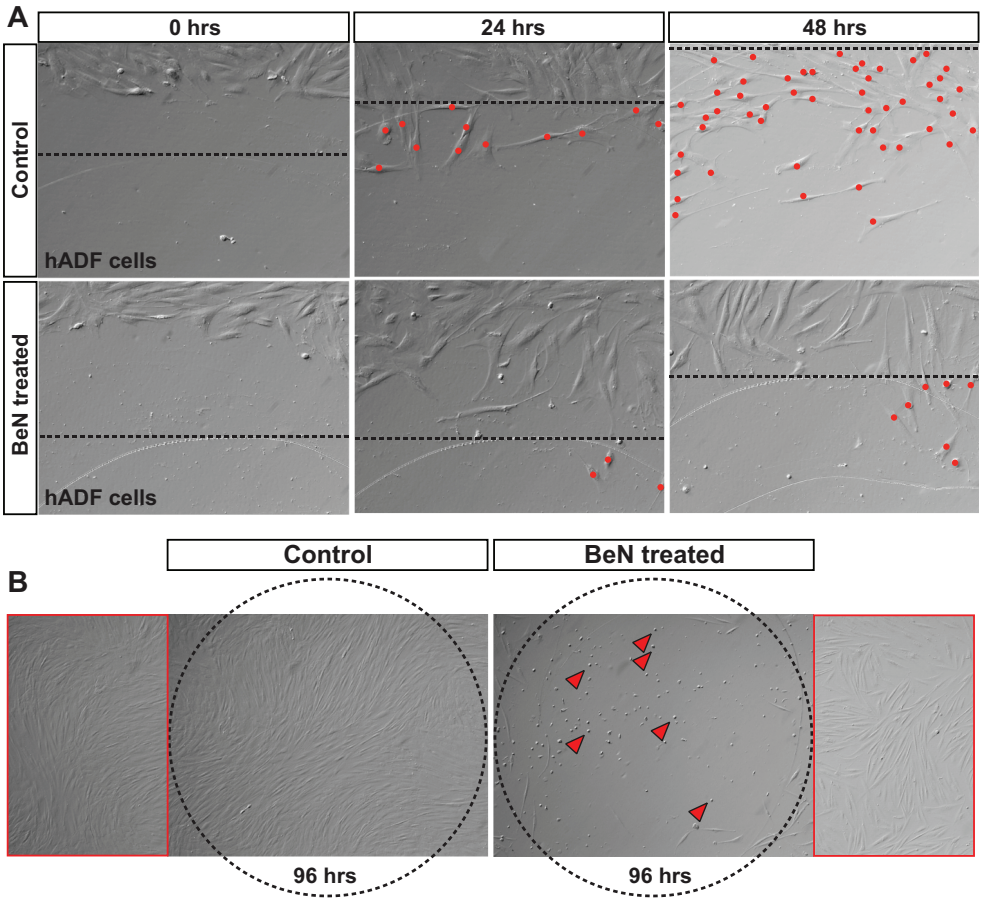

Fig. 9. BeN reduces human dermal fibroblast migration *in vitro*. (A) Migration of human dermal fibroblasts (hADFs) across the inside edge (dotted line) of a circular scratch was tracked over 48 h. Few cells treated with BeN migrated into the *in vitro* wound, whereas control cells completely filled the wound after 96 h (B). BeN treatment reduced cell confluence of hADF cells outside the immediate scratch area (red box). Red arrows show examples of cells in the treatment that have detached from the surface and did not stain with Trypan Blue (data not shown). Data is representative of *n*=6/group.

structures first (Thornton, 1943; Alberch and Gale, 1983). That we observed a bias in patterning defects to proximal structures suggests that the cell cycle defect is secondary to the migration defect.

Previous work with mammalian cells suggested that beryllium has an antagonistic effect on cellular proliferation (Witschi, 1968; Skilleter et al., 1983). Our cell cycle analysis using hADF cells closely mirror those found for rat liver cells exposed to beryllium in that we saw a significantly higher percentage of cells in G1 phase, and a significantly lower percentage of cells in S phase and G2/M phase (Skilleter et al., 1983). Why beryllium exposure appears to block cell cycle progression differently between axolotl and human cells is unclear, although evidence suggests that cell cycle regulation is different between taxa (Tanaka et al., 1997; Pajcini et al., 2010).

Table 1. Flow cytometric analysis of AL1 cells reveals that beryllium nitrate treatment increases the percentage of cells in S phase and decreases the percentage of cells in G2/M, implicating an effect on S phase exit. In contrast, beryllium nitrate treatment of hADF cells produces an increase in G0/G1 cells, implicating an effect on the G1/S transition

Cell cycle phase	Control (mean %± s.e.m.)	BeN-treated (mean % ±s.e.m.)	*P*
AL1			
G0/G1	44.78±0.91	45.95±0.37	0.2977
S	34.31±0.56	39.16±0.64	0.0047
G2/M	20.91±0.36	14.89±0.31	<0.001
hADF			
G0/G1	52.78±0.37	72.42±0.62	<0.001
S	6.19±0.21	2.69±1.35	0.042
G2/M	41.67±0.45	24.89±1.62	<0.001

AL1, *n*=3; hADF, *n*=4.

Importantly, our inclusion of hADF cells in this study shows that beryllium similarly inhibits cell migration in mammalian cells, a fact that is likely to be obscured by *in vivo* studies because of the affect of beryllium on mammalian T-cells (Saltini et al., 1989).

Three classic regeneration studies (Thornton, 1949, 1950, 1951) showed that limb regeneration of *Ambystoma opacum* larvae could be completely inhibited with the application of BeN to a limb stump. Because we did not observe complete inhibition of limb regeneration, our results probably reflect differences in size and stage (larvae versus juvenile) of animals across studies where larval limbs contain far fewer connective tissue fibroblasts. Previous studies showing that beryllium completely inhibits regeneration in other *Ambystoma* species, newts and *Xenopus* larvae (Thornton, 1949, 1950, 1951; Scheuing and Singer, 1957; Tsonis et al., 1991; Mescher et al., 2013), have also documented that the BeN effect is size dependent (for a given concentration), with reduced effects observed on larger organisms (Thornton, 1949). Axolotls used in the present experiments were larger (7-9 cm) compared with larval salamanders and tadpoles used in all previous experiments, suggesting that a similar concentration of BeN may be insufficient to achieve complete inhibition. However, this reduced effect in the context of complete inhibition also revealed a mechanism of action for beryllium in the context of cell migration.

Only one study has proposed a possible mechanism for the beryllium effect in Urodeles: disrupted phosphatidylinositol phosphate (PIP) metabolism (Tsonis et al., 1991). Normal inositol 1,4,5-trisphosphate (IP_3) production rapidly increases and decreases following amputation (Tsonis et al., 1991). $BeSO_4$ exposure caused a 22% decrease in PIP metabolism 30 s after amputation, although $BeSO_4$ exposure at later time points had no effect on PIP metabolism.

Development (2016) 143, 3491-3505 doi:10.1242/dev.134882

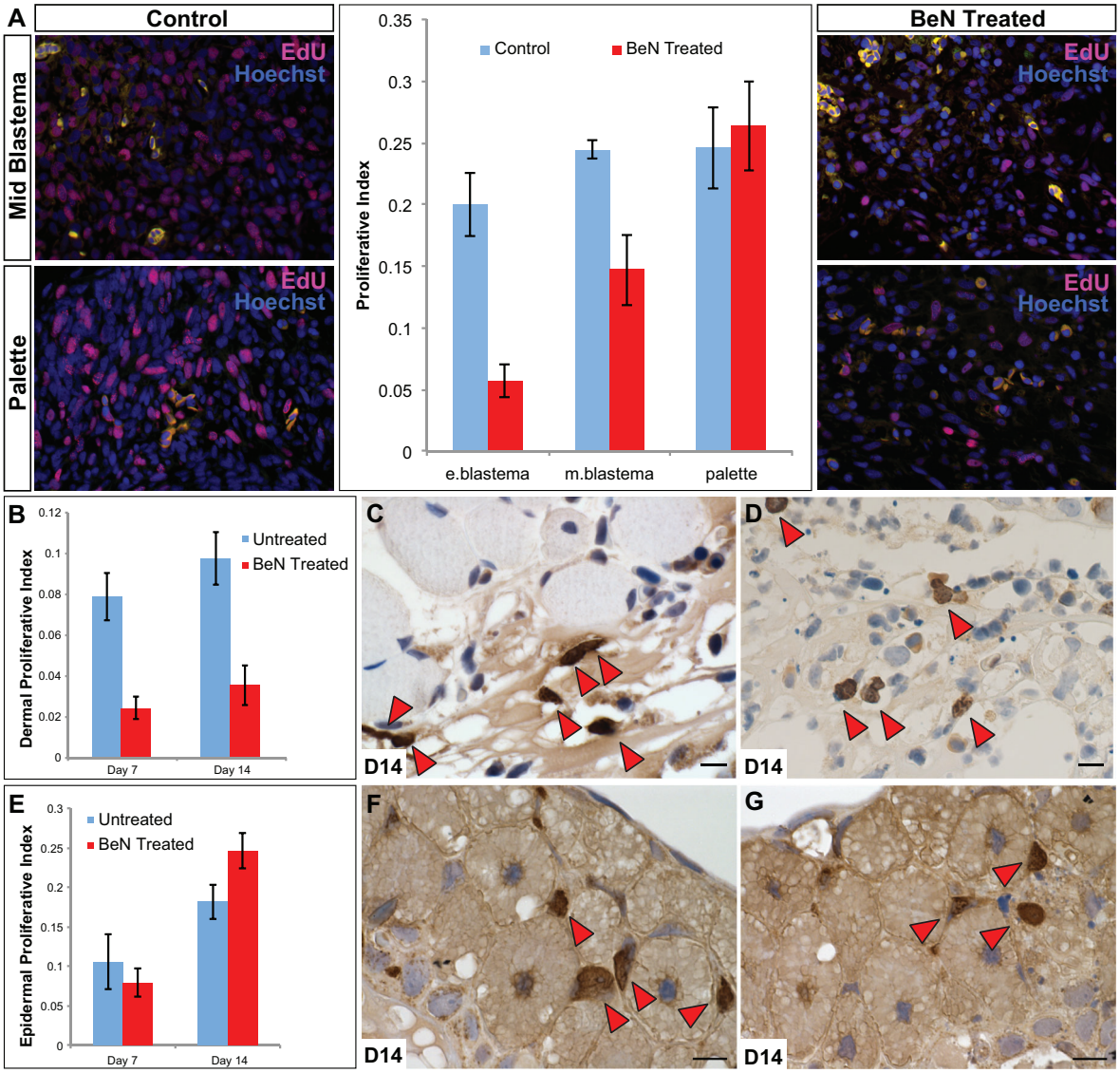

Fig. 10. BeN treatment reduces cell cycle progression *in vivo*. (A) Axolotl limb stumps were treated with 100 mM beryllium nitrate immediately following amputation and labeled with EdU 24 h prior to re-amputation. The difference in the proliferative index of mesenchymal cells between BeN-treated and contralateral control limbs was different by stage (F=4.40, P=0.037, n=5/group). Analyzing each stage, we found a significantly lower proliferative index for BeN-treated limb cells at early- (t=−3.24, P=0.032) and mid-blastema stages (t=−3.08, P=0.037). (B-G) Proliferative index of dermal (B-D) and epidermal cells (E-G) based on BrdU incorporation (red arrows). (B-D) There was a significant reduction in the proliferative index of dermal cells at D7 (t=−4.86, P=0.008, n=5/group) and D14 (t=−3.36, P =0.028, n=5/group) following BeN treatment. (E-G) The proliferative index of epidermal cells (n=5/group) was not significantly different following BeN treatment at D7 or D14 post injury. All data are mean±s.e.m.

Based on *in vitro* work linking IP_3 production to cell cycle activation and proliferation (Berridge, 1987), this study suggested that $BeSO_4$ exposure inhibited cell proliferation, although the authors provided no cell proliferation data. Moreover, cell proliferation does not occur on the timescale observed for PIP metabolism, making this link tenable. Furthermore, Scheuing and Singer's work (1957) with newts seems to contradict the proposed PIP mechanism whereby fully formed blastemas directly infused with BeN inhibited regeneration, which occurred many days after injury when IP_3 levels are low. While it is possible that beryllium has multiple effects on regeneration, both immediately after amputation (PIP-IP3 metabolism) and at a later time (BeN infusion of blastemas), it seems unlikely that beryllium exerts its inhibitory effect through PIP metabolism.

Beryllium has been explored extensively in the context of chronic berylliosis disease whereby inhalation of beryllium dust causes an acute chronic inflammation of the lungs (Newman, 2007). In mammals, this occurs via an acute immune response where beryllium is identified by the major histocompatibility complex and antigen-presenting cells, which themselves stimulate the proliferation and accumulation of $CD4^+$ helper T cells (Saltini et al., 1989). Extended exposure of skin to beryllium also leads to an accumulation of $CD4^+$ cells at the point of contact (Saltini et al., 1989; Fontenot et al., 2002). Interestingly, while much of the T-cell receptor complex has remained conserved between amphibians and mammals (Fellah et al., 1993), functional differences have arisen, specifically in the V-beta region of the T-cell receptor (Fellah et al., 1994). A recent study exposing larval *Xenopus laevis* to beryllium showed that it increased the inflammatory response and attenuated regenerative ability (Mescher et al., 2013). In contrast, our results in salamanders exposing limb amputations and skin wounds to BeN

Development (2016) 143, 3491-3505 doi:10.1242/dev.134882

suggested that a sensitized immune system is not present following BeN exposure. While we observed an edema composed of plasma and erythrocytes consistent with a prolonged hemostatic response, an increase in the number of inflammatory leukocytes was not detected at the treatment site. Recently, depletion of macrophages was shown to inhibit limb regeneration in axolotls, although the extent to which this result was due to the phagocytic versus immune function of macrophages remains unclear (Godwin et al., 2013). While we cannot rule out the effect of macrophage reduction on regeneration, we infer that the effect of this deficit plays a minor role when viewed in the context of our results and the role of fibroblast migration in regeneration. Unfortunately, no reagents exist to reliably detect T-cells or macrophages in salamanders so we could not specifically assay for increased infiltration of these cells, and more importantly, T-cell polarization. Taken together, the data suggest that beryllium can act as an immunostimulatory agent in frogs and mammals, but that immune stimulation does not underlie the inhibitory effect of beryllium on regeneration in salamanders.

Thus, our study shows that beryllium appears to affect endogenous tissue regeneration in two distinct ways: first, through a disruption of cell migration and second, by interrupting cell cycle progression. At present, it remains unclear if BeN operates as a mechanical impairment of the cell's motility systems (extension and reduction of cytoskeleton or integrin binding) or as a sensory impairment of surface receptors and cell signaling machinery. Our experiments have brought to light an interesting phenomenon and underscore the importance of revisiting classic experimental studies in development and regeneration biology. Importantly, this study suggests that beryllium may prove to be a useful tool in testing existing hypotheses about how patterning systems operate during tissue regeneration.

MATERIALS AND METHODS

Animals

Axolotls (*Ambystoma mexicanum*) were acquired from the *Ambystoma* Genetic Stock Center (Lexington, KY, USA) and from our own laboratory colony. Animals were maintained at 17-18°C in modified Holtfreter's solution and maintained on California blackworms (*Lumbriculus variegatus*; J. F. Enterprises). All procedures were conducted in accordance with, and approved by, the University of Kentucky Institutional Animal Care and Use Committee (IACUC Protocol: 2013-1174).

Full-thickness excisional (FTE) wounding and limb amputations

Axolotls (7-8 cm) were anesthetized by full submersion in 0.01% (aqueous) Benzocaine (Sigma). Full-thickness excisional (FTE) wounds through the skin into the dorsal muscle were created using 4 mm biopsy punches (Sklar Instruments). Four dorsal skin wounds were created posterior to the forelimbs and anterior to the hindlimbs (two treatment and two control). In order to measure skin wound area, wounds were photographed and the area of each wound was calculated using Olympus cellSens software. The boundary between uninjured and neo-epidermis was used to define and outline the wound margins. Limb amputations were made through the lower humerus and the extending bone was trimmed. Left limbs and FTE wounds were the treatment group and the wounds on the right served as contralateral controls. Skin wounds were harvested at particular time points post injury based on our previous analysis of skin regeneration in axolotls (Seifert et al., 2012). Limbs were harvested according to well-established morphological stages of regeneration (Wallace, 1981).

Beryllium nitrate (BeN) treatment

Either 100 mM or 140 mM beryllium nitrate solutions were prepared by diluting a stock solution (35% w/v) (Sigma) in distilled water. A 140 mM concentration was used in the original experiments (Thornton, 1947) and we determined that 140 mM and 100 mM produced the same result in our animals. Following a single limb amputation or FTE wound, animals were submersed in 100 mM BeN for 2 min, after which they were continually rinsed in running tap water for 10 min. After rinsing, either the contralateral limb or a second wound corresponding to the mirror position across the dorsal midline was made. In this way, each animal served as its own control. For *in vitro* experiments, three dilutions of BeN were prepared (1 mM, 10 mM and 100 mM) and tested for cytotoxicity. Cytotoxicity and cell death was assessed using the vital dye Trypan Blue (Hyclone). Based on these tests, 10 mM BeN was used in all subsequent cell culture experiments.

Histology and immunohistochemistry

Freshly harvested tissues were fixed in 10% neutral buffered formalin (NBF) (American Master Tech Scientific) overnight (~16-24 h), washed in phosphate buffered saline (PBS) three times, dehydrated in 70% ethanol and processed for paraffin embedding. Limb samples were decalcified in 10% EDTA (pH 7.4) for 3 days at room temperature with daily changes before processing. Tissue samples were sectioned at 5 µm. Tissue sections were stained with Masson's trichrome (Richard-Allen Scientific), Picrosirius Red (American Master Tech) or Alcian Blue (Sigma). For frozen sections, samples were fixed for 1 h in 10% NBF at 4°C, washed in PBS, equilibrated in 30% sucrose and OCT freezing medium, and rapidly frozen on dry ice for storage at −20°C. Frozen sections were cut at 12 µm. Immunohistochemistry was performed as previously described (Seifert et al., 2012) (see supplementary Materials and Methods for full details of antibodies and antigen retrieval methods). BrdU and EdU immunohistochemistry was performed as previously described (Calve et al., 2010; Monaghan et al., 2014).

Cell lines and circular scratch assays

Two cell types were analyzed *in vitro*: human adult dermal fibroblasts (hADF) (gift from Karen Echeverri, acquired from Lonza Group Ltd) and axolotl fibroblasts (AL1) (gift from Stéphane Roy, Université de Montréal). All available AL1 cells were maintained with a low level of contamination, whereas hADF cells were contamination free. Both cell types were expanded in T-25 and T-75 cell culture flasks (Greiner Bio-One). AL1 cells were grown in medium containing 60% L-15 (Leibovitz) medium without L-glutamine (Sigma), 32% ddH_2O, 5% fetal bovine serum (FBS) (GE Healthcare Bio-Sciences), 1% insulin/selenium/transferrin (Life Technologies), 1% penicillin/streptomycin/amphotericin-b (Sigma) and 1% L-glutamine (Life Technologies). hADF cells were grown in medium containing 88% Dulbecco's modified Eagle medium/F-12 (DMEM) (Life Technologies), 10% FBS (GE Healthcare Bio-Sciences), 1% insulin/selenium/transferrin (Life Technologies), 1% penicillin/streptomycin/amphotericin-b (Sigma-Aldrich). Cells were passaged at 70-80% confluency. Cells were passaged by rinsing with Dulbecco's PBS solution (DPBS) (Life Technologies), treating with 0.25% Trypsin-ETDA (Life Technologies) for 3-5 min, and centrifuging for 3 min at 3000 rpm. Each cell line was split 1:2 or 1:3 into new flasks with fresh medium until a large stock of cells was obtained. Both cell types were grown in 12-well tissue culture treated plates and allowed to reach ~80% confluency prior to any procedure. Half of the wells were treated with 10 mM beryllium nitrate for 2 min and rinsed three times with DPBS. An *in vitro* wound was created with a cotton tip applicator in the center of each well. Cells were tracked and images were taken every 12 or 24 h up to 96 h (hADF cells) or 14 days (AL1 cells) following treatment.

Analysis of cell death, proliferation and cell cycle progression

Cells undergoing apoptosis were detected using a TUNEL assay employing a GFP tag (Roche Life Sciences). A cell death index was calculated for dermal cells expressing GFP divided by the total number of cells (stained with Hoechst 1:10,000 stock, Invitrogen) present in the same counting field. To detect cells in S phase, 100 mg/kg BrdU or 10 µg/g EdU was IP injected into axolotls and tissues were harvested after 24 h. Detection was carried out on formalin-fixed, paraffin-embedded tissue sections and cells were visualized using DAB (BrdU) or an Alexa Fluor azide (Invitrogen) (as detailed in supplementary Materials and Methods).

Calculation of the proliferative index (PI) for BrdU-marked cells was conducted on images taken from three random fields of view at 40× magnification. The PI was equal to the number of $BrdU^+$ cells divided by the total number of cells. The calculation of PI for EdU^+ cells within the

Development (2016) 143, 3491-3505 doi:10.1242/dev.134882

regenerating limb was conducted at the same magnification from two random fields of view and followed the same mathematical formula. Calculations were carried out with cellSens microscopy software (Olympus).

For *in vitro* experiments, AL1 and hADF cells were used (see above). For the cell cycle progression assay, cultured cells were fixed in complete darkness with cold 70% ethanol for 1 h, centrifuged at 2000 rpm for 10 min, rinsed in 1× PBS and centrifuged again until a pellet formed, treated with 1 mg/ml propidium iodide and 10 mg/ml RNase A (Sigma) in 1× PBS, and incubated in darkness at 37°C for 30 min. Cells were not synchronized prior to fixation. Samples were run on a Becton Dickinson FACSCalibur (BD Biosciences) within 4 h of preparation. Cells containing DNA labeled with propidium iodide were sorted into four groups based on their relative fluorescence and DNA content frequency histograms were generated. Cells with luminosity less than 1× were considered apoptotic, cells with 1× luminosity had a normal level of DNA and were considered to be in G0/G1, cells between 1× and 2× luminosity were undergoing DNA replication (S phase) and cells with 2× luminosity had twice the amount of DNA and were considered in G2/M. Cells that fell outside of the acceptable range of fluorescence were not counted. Each group of cells (biological replicate) was analyzed independently and the data was considered clean if there were two narrow and distinct luminosity peaks. Modfit software was used to deconvolute the frequency histograms to obtain percentage of cells in each stage for each biological replicate. The percentage of cells at each stage was averaged across all replicates (AL1, n=3 and hADF, n=4) and the standard error was calculated for each phase accordingly.

GFP tissue transplantations

To track dermal fibroblasts *in vivo*, full-thickness skin comprising dermis and epidermis was extracted from the dorsal flank of axolotls constitutively expressing GFP in all cell types (see Fig. 6A) (Sobkow et al., 2006). Identical injuries were made on WT individuals of approximate age and size. Two wounds were made on WT animals: one for treatment with BeN and the other as a control. A GFP tissue graft was placed into the open wound on WT animals and attached with Vetbond (3 M). Wounds were allowed to heal and integrate with host tissue for 2 weeks. After 2 weeks, a second injury was made in the center of the 8 mm GFP transplant using a 4 mm biopsy punch. The anterior-most transplant of each animal was injured first and treated with 100 mM BeN for 2 min followed by a 10 minute rinse (see above). A biopsy was taken from the remaining transplant and this wound served as the control. Each transplant was harvested 14 days later using an 8 mm biopsy punch and preserved for cryosectioning. Using this methodology, any GFP^+ cells in the wound bed would represent fibroblasts because: (1) GFP^+ epidermis in the original donor tissue was covered and replaced by host WT epidermis and epidermal cells do not invade the mesenchymal compartment of the wound bed, (2) circulating host blood and immune cells were not GFP^+ and (3) the majority of fibroblasts that infiltrate the injury site are locally derived from a 200-500 µm area immediately surrounding the injury (Mchedlishvili et al., 2007), and these constitutively expressed GFP.

To analyze fibroblast migration in regenerating limbs, we transplanted full-thickness GFP^+ skin cuffs (epidermis and dermis) from the forelimb of a GFP animal onto WT forelimbs in the same position so as to maintain positional continuity around the limb (see Fig. 6E). Rectangular skin cuffs were taken from the mid dorsal region to the mid ventral region on the posterior side of each limb. We carefully maintained the positional identity of each GFP cuff before applying it to the WT individuals and allowed them to heal for 14 days before amputating each limb through the center of the transplants. The left limb was always amputated first and the animal treated with beryllium nitrate for 2 min followed by a 10 min rinse. The control limb was then amputated and each animal was allowed to heal until the desired stage was reached on the control limb, at which point limbs were re-amputated just proximal to the transplant and prepared for cryosectioning.

Microscopy and image acquisition

Bright-field images were taken on a BX53 light microscope (Olympus) using a DP80 CCD camera (Olympus). Whole mount images were taken on an SZX10 light microscope (Olympus) using a DP73 CCD camera (Olympus). All *in vitro* images were taken on an IX71 inverted microscope (Olympus) with a DP72 CCD camera (Olympus).

Statistics

Basic comparisons between control and experimental groups were conducted using JMP software (SAS, Cary, NC) to report standard deviation, standard error of the mean and to conduct statistical tests. Paired *t*-tests were used to measure differences in wound area of FTE skin wounds and to quantify differences in numbers of leukocytes (in skin and limb injuries because treatment and control wounds were made on the same individuals). A chi-square test was used to determine if beryllium treatment significantly altered cell cycle progression in AL1 and hADF cells. Unpaired *t*-tests were used as a *post hoc* analysis to test for differences among the percentage of AL1 and hADF cells in various stages of the cell cycle. Unpaired *t*-tests were also used to measure differences in the number of migrating fibroblasts in the regenerating dermis. A one-way ANOVA was used to analyze differences in apoptosis and cellular proliferation by taking the difference between paired control and treatment groups at each time point. All tests performed were two-tailed. The level of significance was set at 0.05.

Acknowledgements

We would like to thank Dr Jeramiah Smith for constructive discussions during this study and for critically reading the manuscript. We also thank Drs Karen Echeverri, Stéphane Roy and Edmund Rucker for techniques and resources for cell culture, Greg Bauman and the University of Kentucky Flow Cytometry and Cell Sorting Core Facility for FACS assistance and Dr Antony Athippozhy, Melvin Woodcock and Kevin Kump for assistance with statistical analysis of the data.

Competing interests

The authors declare no competing or financial interests.

Author contributions

A.B.C and A.W.S developed the project, designed and carried out the experiments and wrote the manuscript.

Funding

This work was supported by the University of Kentucky Office of Research.

Supplementary information

Supplementary information available online at
http://dev.biologists.org/lookup/doi/10.1242/dev.134882.supplemental

References

Alberch, P. and Gale, E. A. (1983). Size dependence during the development of the amphibian foot. Colchicine-induced digital loss and reduction. *J. Embryol. Exp. Morphol.* **76**, 177-197.

Asahina, K., Obara, M. and Yoshizato, K. (1999). Expression of genes of type I and type II collagen in the formation and development of the blastema of regenerating newt limb. *Dev. Dyn.* **216**, 59-71.

Berridge, M. J. (1987). Inositol trisphosphate and diacylglycerol: two interacting second messengers. *Annu. Rev. Biochem.* **56**, 159-193.

Brockes, J. P. (1987). The nerve dependence of amphibian limb regeneration. *J. Exp. Biol.* **132**, 79-91.

Bryant, S. V. (1976). Regenerative failure of double half limbs in *Notophthalmus viridescens*. *Nature* **263**, 676-679.

Bryant, S. and Gardiner, D. (1989). Position-dependent growth control and pattern formation in limb regeneration. In *Recent Trends in Regeneration Research* (ed. V. Kiortsis, S. Koussoulakos and H. Wallace), pp. 377-390. New York: Springer.

Butler, E. G. and Ward, M. B. (1967). Reconstitution of the spinal cord after ablation in adult Triturus. *Dev. Biol.* **15**, 464-486.

Calve, S., Odelberg, S. J. and Simon, H.-G. (2010). A transitional extracellular matrix instructs cell behavior during muscle regeneration. *Dev. Biol.* **344**, 259-271.

Carlson, B. M. (1974). Morphogenetic interactions between rotated skin cuffs and underlying stump tissues in regenerating axolotl forelimbs. *Dev. Biol.* **39**, 263-285.

Chalkley, D. T. (1954). A quantitative histological analysis of forelimb regeneration in Triturus viridescens. *J. Morphol.* **94**, 21-70.

Crawford, K. and Stocum, D. L. (1988a). Retinoic acid proximalizes level-specific properties responsible for intercalary regeneration in axolotl limbs. *Development* **104**, 703-712.

Crawford, K. and Stocum, D. L. (1988b). Retinoic acid coordinately proximalizes regenerate pattern and blastema differential affinity in axolotl limbs. *Development* **102**, 687-698.
Echeverri, K. and Tanaka, E. M. (2005). Proximodistal patterning during limb regeneration. *Dev. Biol.* **279**, 391-401.
Eguchi, G., Eguchi, Y., Nakamura, K., Yadav, M. C., Millán, J. L. and Tsonis, P. A. (2011). Regenerative capacity in newts is not altered by repeated regeneration and ageing. *Nat. Commun.* **2**, 384.
Endo, T., Bryant, S. V. and Gardiner, D. M. (2004). A stepwise model system for limb regeneration. *Dev. Biol.* **270**, 135-145.
Fellah, J. S., Kerfourn, F., Guillet, F. and Charlemagne, J. (1993). Conserved structure of amphibian T-cell antigen receptor beta chain. *Proc. Natl. Acad. Sci.* **90**, 6811-6814.
Fellah, J. S., Kerfourn, F. and Charlemagne, J. (1994). Evolution of T cell receptor genes. Extensive diversity of V beta families in the Mexican axolotl. *J. Immunol.* **153**, 4539-4545.
Fontenot, A. P., Maier, L. A., Canavera, S. J., Hendry-Hofer, T. B., Boguniewicz, M., Barker, E. A., Newman, L. S. and Kotzin, B. L. (2002). Beryllium skin patch testing to analyze T cell stimulation and granulomatous inflammation in the lung. *J. Immunol.* **168**, 3627-3634.
Globus, M. and Vethamany-Globus, S. (1977). Transfilter mitogenic effect of dorsal root ganglia on cultured regeneration blastemata, in the newt, Notophthalmus viridescens. *Dev. Biol.* **56**, 316-328.
Globus, M., Vethamany-Globus, S. and Lee, Y. C. (1980). Effect of apical epidermal cap on mitotic cycle and cartilage differentiation in regeneration blastemata in the newt, *Notophthalmus viridescens*. *Dev. Biol.* **75**, 358-372.
Godwin, J. W., Pinto, A. R. and Rosenthal, N. A. (2013). Macrophages are required for adult salamander limb regeneration. *Proc. Natl. Acad. Sci. USA* **110**, 9415-9420.
Gulati, A. K., Zalewski, A. A. and Reddi, A. (1983). An immunofluorescent study of the distribution of fibronectin and laminin during limb regeneration in the adult newt. *Dev. Biol.* **96**, 355-365.
Jones, S. L., Wang, J., Turck, C. W. and Brown, E. J. (1998). A role for the actin-bundling protein l-plastin in the regulation of leukocyte integrin function. *Proc. Natl. Acad. Sci.* **95**, 9331-9336.
Kim, W.-S. and Stocum, D. L. (1986). Retinoic acid modifies positional memory in the anteroposterior axis of regenerating axolotl limbs. *Dev. Biol.* **114**, 170-179.
Kragl, M., Knapp, D., Nacu, E., Khattak, S., Maden, M., Epperlein, H. H. and Tanaka, E. M. (2009). Cells keep a memory of their tissue origin during axolotl limb regeneration. *Nature* **460**, 60-65.
Lheureux, E. (1975a). Nouvelles données sur les rôles de la peau et des tissues internes dans la régénération du membre du triton *Pleurodeles waltlii*, Michah (amphibian urodèle). *Wilhelm Roux. Arch. Entwickl. Mech. Org.* **776**, 285-301.
Lheureux, E. (1975b). Régénération des membres irradiés de Pleurodeles waltlii Michah. (Urodčle). Influence des qualités et orientations des greffons non irradies. *Wilhelm Roux. Arch. Entwickl. Mech. Org.* **176**, 303-327.
Lheureux, E. (1977). Importance des associations de tissus du membre dans le développement des membres surnuméraires induits par déviation de nerf chez le Triton *Pleurodeles waltlii* Michah. *J. Embryol. Exp. Morphol.* **38**, 151-173.
Lheureux, E. and Carey, F. (1987). The irradiated epidermis inhibits newt limb regeneration by preventing blastema growth. A histological study. *Biol. Struct. Morphog.* **1**, 49-57.
Ludolph, D. C., Cameron, J. A. and Stocum, D. L. (1990). The effect of retinoic acid on positional memory in the dorsoventral axis of regenerating axolotl limbs. *Dev. Biol.* **140**, 41-52.
Maden, M. (1978). Neurotrophic control of the cell cycle during amphibian limb regeneration. *J. Embryol. Exp. Morphol.* **48**, 169-175.
Maden, M. (1983). A test of the predictions of the boundary model regarding supernumerary limb structure. *J. Embryol. Exp. Morphol.* **76**, 147-155.
Maden, M. and Wallace, H. (1976). How X-rays inhibit amphibian limb regeneration. *J. Exp. Zool.* **197**, 105-113.
Mchedlishvili, L., Epperlein, H. H., Telzerow, A. and Tanaka, E. M. (2007). A clonal analysis of neural progenitors during axolotl spinal cord regeneration reveals evidence for both spatially restricted and multipotent progenitors. *Development* **134**, 2083-2093.
Mescher, A. L. (1976). Effects on adult newt limb regeneration of partial and complete skin flaps over the amputation surface. *J. Exp. Zool.* **195**, 117-127.
Mescher, A. L., Neff, A. W. and King, M. W. (2013). Changes in the inflammatory response to injury and its resolution during the loss of regenerative capacity in developing xenopus limbs. *PloS ONE* **8**, e80477.
Monaghan, J. R., Stier, A. C., Michonneau, F., Smith, M. D., Pasch, B., Maden, M. Seifert, A. W. (2014). Experimentally induced metamorphosis in axolotls reduces regenerative rate and fidelity. *Regeneration* **1**, 2-14.
Morgan, T. H. (1901). *Regeneration*. New York, London: The Macmillan Company; Macmillan & Co., ltd.
Muneoka, K., Fox, W. F. and Bryant, S. V. (1986). Cellular contribution from dermis and cartilage to the regenerating limb blastema in axolotls. *Dev. Biol.* **116**, 256-260.
Nardi, J. B. and Stocum, D. L. (1984). Surface properties of regenerating limb cells: evidence for gradation along the proximodistal axis. *Differentiation* **25**, 27-31.
Needham, A. (1941). Some experimental biological uses of the element beryllium (glucinum). In *Proceedings of the Zoological Society of London*, vol. 111, pp. 59-85. Oxford: Blackwell Publishing.
Newman, L. S. (2007). Immunotoxicology of beryllium lung disease. *Environ. Health Prev. Med.* **12**, 161-164.
Onda, H., Goldhamer, D. J. and Tassava, R. A. (1990). An extracellular matrix molecule of newt and axolotl regenerating limb blastemas and embryonic limb buds: immunological relationship of MT1 antigen with tenascin. *Development* **108**, 657-668.
Pajcini, K. V., Corbel, S. Y., Sage, J., Pomerantz, J. H. and Blau, H. M. (2010). Transient inactivation of Rb and ARF yields regenerative cells from postmitotic mammalian muscle. *Cell Stem Cell* **7**, 198-213.
Pulido, M. D. and Parrish, A. R. (2003). Metal-induced apoptosis: mechanisms. *Mutat. Res.* **533**, 227-241.
Salley, J. D. and Tassava, R. A. (1981). Responses of denervated adult newt limb stumps to reinnervation and reinjury. *J. Exp. Zool.* **215**, 183-189.
Saltini, C., Winestock, K., Kirby, M., Pinkston, P. and Crystal, R. G. (1989). Maintenance of alveolitis in patients with chronic beryllium disease by beryllium-specific helper T cells. *N. Engl. J. Med.* **320**, 1103-1109.
Satoh, A., Gardiner, D. M., Bryant, S. V. and Endo, T. (2007). Nerve-induced ectopic limb blastemas in the Axolotl are equivalent to amputation-induced blastemas. *Dev. Biol.* **312**, 231-244.
Scheuing, M. R. and Singer, M. (1957). The effects of microquantitles of beryllium ion on the regenerating forelimb of the adult newt, Triturus. *J. Exp. Zool.* **136**, 301-327.
Schotté, O. E. and Butler, E. G. (1941). Morphological effects of denervation and amputation of limbs in urodele larvae. *J. Exp. Zool.* **87**, 279-322.
Seifert, A. W. and Maden, M. (2014). New insights into vertebrate skin regeneration. *Int. Rev. Cell Mol. Biol.* **310**, 129-169.
Seifert, A. W., Monaghan, J. R., Voss, S. R. and Maden, M. (2012). Skin regeneration in adult axolotls: a blueprint for scar-free healing in vertebrates. *PLoS ONE* **7**, e32875.
Singer, M. (1951). Induction of regeneration of forelimb of the frog by augmentation of the nerve supply. *Proc. Soc. Exp. Biol. Med.* **76**, 413-416.
Singer, M. (1952). The influence of the nerve in regeneration of the amphibian extremity. *Q Rev. Biol.* **27**, 169-200.
Singer, M., Flinker, D. and Sidman, R. L. (1956). Nerve destruction by colchicine resulting in suppression of limb regeneration in adult Triturus. *J. Exp. Zool.* **131**, 267-299.
Singh, B. N., Doyle, M. J., Weaver, C. V., Koyano-Nakagawa, N. and Garry, D. J. (2012). Hedgehog and Wnt coordinate signaling in myogenic progenitors and regulate limb regeneration. *Dev. Biol.* **371**, 23-34.
Skilleter, D. N., Price, R. J. and Legg, R. F. (1983). Specific G1-S phase cell cycle block by beryllium as demonstrated by cytofluorometric analysis. *Biochem. J.* **216**, 773-776.
Slack, J. M. (1983). Positional information in the forelimb of the axolotl: properties of the posterior skin. *J. Embryol. Exp. Morphol.* **73**, 233-247.
Sobell, H. M. (1985). Actinomycin and DNA transcription. *Proc. Natl. Acad. Sci.* **82**, 5328-5331.
Sobkow, L., Epperlein, H.-H., Herklotz, S., Straube, W. L. and Tanaka, E. M. (2006). A germline GFP transgenic axolotl and its use to track cell fate: dual origin of the fin mesenchyme during development and the fate of blood cells during regeneration. *Dev. Biol.* **290**, 386-397.
Spallanzani, L. (1769). An essay on animal reproductions. Translated from the Italian by T. Becket and P.A. de Hondt.
Stocum, D. (1978). Regeneration of symmetrical hindlimbs in larval salamanders. *Science* **200**, 790-793.
Stocum, D. L. (2011). The role of peripheral nerves in urodele limb regeneration. *Eur. J. Neurosci.* **34**, 908-916.
Stocum, D. L. and Dearlove, G. E. (1972). Epidermal-mesodermal interaction during morphogenesis of the limb regeneration blastema in larval salamanders. *J. Exp. Zool.* **181**, 49-61.
Tanaka, E. M., Gann, A. A., Gates, P. B. and Brockes, J. P. (1997). Newt myotubes reenter the cell cycle by phosphorylation of the retinoblastoma protein. *J. Cell Biol.* **136**, 155-165.
Thornton, C. S. (1943). The effect of colchicine on limb regeneration in larval Amblystoma. *J. Exp. Zool.* **92**, 281-295.
Thornton, C. S. (1947). Some effects of beryllium nitrate on regeneration. *Anat Rec.* **99**, 631.
Thornton, C. S. (1949). Beryllium inhibition of regeneration. 1. Morphological effects of beryllium on amputated fore limbs of larval amblystoma. *J. Morphol.* **84**, 459-493.
Thornton, C. S. (1950). Beryllium inhibition of regeneration. 2. Localization of the beryllium effect in amputated limbs of larval amblystoma. *J. Exp. Zool.* **114**, 305-333.
Thornton, C. S. (1951). Beryllium inhibition of regeneration. 3. Histological effects of beryllium on the amputated fore limbs of amblystoma larvae. *J. Exp. Zool.* **118**, 467-493.
Todd, T. (1823). On the process of reproduction of the members of the aquatic salamander. *Q. J. Sci. Lit. Arts* **16**, 84-96.

Development (2016) 143, 3491-3505 doi:10.1242/dev.134882

Tsonis, P. A., English, D. and Mescher, A. L. (1991). Increased content of inositol phosphates in amputated limbs of axolotl larvae, and the effect of beryllium. *J. Exp. Zool.* **259**, 252-258.
Wallace, H. (1981). *Vertebrate Limb Regeneration.* New York: Wiley.
Wallace, H. and Maden, M. (1976). The cell cycle during amphibian limb regeneration. *J. Cell Sci.* **20**, 539-547.
Witschi, H. (1968). Inhibition of deoxyribonucleic acid synthesis in regenerating rat liver by beryllium. *Lab. Invest.* **19**, 67-70.